Frankiamide, a Highly Unusual Macrocycle Containing the Imide and Orthoamide Functionalities from the Symbiotic Actinomycete *Frankia*

Karel D. Klika,[†] J. Pasi Haansuu,[‡] Vladimir V. Ovcharenko,[†] Kielo K. Haahtela,[‡] Pia M. Vuorela,[§] and Kalevi Pihlaja*[,†]

Department of Chemistry, University of Turku, FIN-20014 Turku, Finland, Department of Biosciences, Division of General Microbiology, University of Helsinki, and Department of Pharmacy, Viikki Drug Discovery Technology Center, University of Helsinki, FIN-00014 Helsinki, Finland

kalevi.pihlaja@utu.fi

Received December 26, 2000

Frankia is a symbiotic actinomycete that forms nitrogen-fixing root nodules in actinorhizal plants such as alder (*Alnus* sp.) and *Casuarina* sp., but it also commonly resides in soils lacking host plants.[1−4] Recently, it has been shown that *Frankiae* frequently produce compounds with antimicrobial activity against Gram-positive *Brevibacillus laterosporus* and Gram-negative *Pseudomonas solanacearum*.[5,6] These compounds may have a defensive role and, in addition to the iron-chelating siderophores, plant hormones, and hydrolyzing enzymes also produced by *Frankiae*, evidently assist *Frankia*, a slow growing microbe, to survive in nonsymbiotic conditions.[7−11] Both *Frankia* strains G2 (ORS 020604) and ANP 190107 are also known to synthesize benzonaphthacene quinone metabolites that are structurally related to the antimicrobial compounds produced by some *Streptomyces* sp.,[12−15] and two of these quinones were shown to possess biological activity by inhibiting the mitochondria of the yeast *Candida lipolytica*, the function of the respiratory chain in *Paracoccus denitrificans*, and the growth of Gram-positive *Arthrobacter globiformis*, the deuteriomycete *Fusarium decemcellulare*, and *Candida lipolytica*.[16] Calcium channel antagonists, commonly used drugs for the treatment of cardiovascular disorders, have as their primary targets the slowly deactivating, low-activation threshold voltage-sensitive calcium channels (VOCCs), and by their action Ca^{2+} influx is inhibited, resulting in the relaxation of vascular smooth muscle. Plant extracts containing phenolic compounds are known to affect the function of VOCCs,[17] and several *Frankia* culture broth extracts have been shown to considerably inhibit Ca^{2+} fluxes in clonal rat pituitary GH_4C_1 cells.[5] Recently, we isolated a particular *Frankia* strain, AiPs1, from a stand of Finnish Scots pine (*Pinus sylvestris* L.).[2] After TLC fractionation of the microbial culture broth extract, only one antimicrobially active fraction was identified from which, using RP-TLC, was isolated a compound that inhibited the growth of several pathogenic fungi and Gram-positive bacteria. Moreover, this compound was also found to exhibit significant inhibition of $^{45}Ca^{2+}$ fluxes in clonal rat pituitary GH_4C_1 cells. The isolation procedure of the compound, together with the cultivation of the *Frankia* strain and assessment of the bioactivity of the isolated compound, are described in detail elsewhere,[18] while this report describes the structure of the isolated compound (**1**), a novel macrocycle, which is depicted in Figure 1. To reflect both its origin and to allude to the inherent functionalities present within the system, we have dubbed **1** "frankiamide".

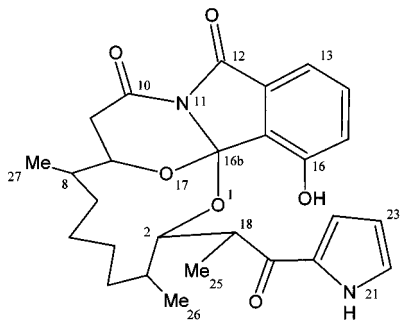

Figure 1. The structure of frankiamide (**1**) together with the numbering system in use. Note that the stereochemistry is unknown and is not inferred.

The structural elucidation of **1** only followed readily from NMR after some initial problems and the final realization of the molecular weight as 480 amu (not trivial, see below) and the resulting formula from HRMS analysis as $C_{27}H_{32}N_2O_6$. In methanol solution the compound exists as two readily interconverting forms (as evidenced by EXSY spectra) in the ratio of 3:1. That this interconversion was intricately linked to the concentration of Na^+ ions was demonstrated by the addition of aqueous Na_2HPO_4 to the NMR sample, resulting in the shifting of the equilibrium further to one form. This dynamic process increased the complexity of the spectra, both by the presence of a greater number of signals and by the breadth of the peaks themselves, and made the

* Ph: 358-(2)-3336767. Fax: 358-(2)-3336750.
[†] University of Turku.
[‡] Department of Biosciences, Division of General Microbiology, University of Helsinki.
[§] Department of Pharmacy, Viikki Drug Discovery Technology Center, University of Helsinki.

(1) Huss-Danell, K.; Frej, A. K. *Plant Soil* **1986**, *90*, 407.
(2) Maunuksela, L.; Zepp, K.; Koivula, T.; Zeyer, J.; Haahtela K.; Hahn, D. *Microbiol. Ecol.* **1998**, *28*, 11.
(3) Smolander, A. *Plant Soil* **1990**, *121*, 1.
(4) Smolander, A.; Rönkkö, R.; Nurmiaho-Lassila, E.-L.; Haahtela, K. *Can. J. Microbiol.* **1990**, *36*, 649.
(5) Haansuu, P.; Vuorela, P.; Haahtela, K. *Pharm. Pharmacol. Lett.* **1999**, *9*, 1.
(6) Lang, L. *For. Res.* **1999**, *12*, 47.
(7) Arahou, M.; Diem, H. G.; Sasson, A. *World J. Microbiol. Biotech.* **1998**, *14*, 31.
(8) Aronson, D. B.; Boyer, G. L. *Soil Biol. Biochem.* **1994**, *26*, 561.
(9) Mansour, S. R.; El Melegy, S. A. *Egypt. J. Microbiol.* **1997**, *32*, 423.
(10) Safo-Sampah, S.; Torrey, J. G. *Plant Soil* **1988**, *112*, 89.
(11) Séguin, A.; Lalonde, M. *Plant Soil* **1989**, *118*, 221.
(12) Gerber, N. N.; Lechevalier, M. P. *Can. J. Chem.* **1984**, *62*, 2818.
(13) Gomi, S.; Sasaki, T.; Itoh, J.; Sezaki, M. *J. Antibiot.* **1988**, *41*, 425.
(14) Rickards, R. W. *J. Antibiot.* **1989**, *42*, 336.
(15) Takeda, U.; Okada, T.; Takagi, M.; Gomi, S.; Itoh, J.; Sezaki, M.; Ito, M.; Miyadoh, S.; Shomura, T. *J. Antibiot.* **1988**, *41*, 417.
(16) Medentsev, A. G.; Baskunov, B. P.; Stupar, O. S.; Nefedova, M. Y.; Akimenko V. K. *Biokhimiya* **1989**, *54*, 926.
(17) Vuorela, H.; Vuorela, P.; Törnquist, K.; Alaranta, S. *Phytomedicine* **1997**, *4*, 167.
(18) Haansuu, J. P.; Klika, K. D.; Söderholm, P. P.; Ovcharenko, V. V.; Pihlaja, K.; Haahtela, K. K.; Vuorela, P. M. *J. Ind. Microbiol. Biot.* **2001**, submitted for publication

10.1021/jo001789z CCC: $20.00
Published on Web 05/04/2001

structural analysis more difficult. Although the addition of Na_2HPO_4 improved matters, it did not sufficiently alleviate the problem; neither did slowing the rate of exchange by lowering the temperature (−50 °C), and a sufficient increase in temperature to attain an averaged spectrum (>150 °C) only led to the rapid decomposition of the compound. In chloroform solution, however, this dynamic equilibrium was even more biased (>10:1). The interconversion was slower by comparison, and the resulting spectra were thus much more manageable; for this reason the NMR results are reported for $CDCl_3$ solution. This behavior was also reflected in the HPLC analysis, which generally showed extremely broad peaks with front-end tailing, but fractions across the peak were assessed to be the same interconverting species by exchange spectra and by admixture, i.e., different fractions merely represented different positions of the equilibrium. Similarly, the chromatographic behavior could also be considerably improved by the addition of Na_2HPO_4 to the eluent.

For the structural elucidation, gross sections of the molecule were readily apparent by NMR, such as the presence of a 2-substituted pyrrole ring (carbonyl adjacent to the ring), which was evident by the ^1H chemical shifts and ^1H coupling constants together with long-range $^1H-^{13}C$ correlations. Mass spectral analysis also strongly inferred the presence of a carbonyl α to a pyrrole ring. The 1,2,3-trisubstituted phenyl ring (carbonyl adjacent to the ring at position 1, carbon at position 2, and oxygen at position 3) was evident by the ^1H chemical shifts, ^1H coupling constants, ^{13}C chemical shifts, and long-range $^1H-^{13}C$ correlations. The directly attached oxygen was proven to be a phenol group as a positive was obtained in a modified Folin−Ciocalteu phenol test[19] (the other five oxygens were also discounted as bearing a proton, for three oxygens were present as carbonyls and the other two were each singly bound to two carbons). Finally, the alkyl segments proved to be all contained within one branched but unbroken alkyl chain. Tracing the alkyl chain from any distinct point (α to the carbonyls or the oxygen links) only led into the "alkyl forest", and only methylene alkyl fragments were left unassigned, which were clearly only attached to other alkyl fragments by their chemical shifts, thus providing the deduction for the one alkyl chain. One of the carbonyls at the end of this chain was also shown to be the same carbonyl α to the pyrrole ring. Thus, what was remaining was an interesting quaternary carbon at 96.4 ppm and a tertiary nitrogen at −161.5 ppm; both were easily placed as a result of the observation of suitable long-range correlations. Since the long-range correlations, both $^1H-\{^{13}C\}$ and $^1H-\{^{15}N\}$ HMBC experiments and $^{13}C-\{^1H\}$ selective INEPT, played, as expected, such an instrumental role in placing these fragments together, the decisive correlations are depicted in Figure 2.

By default, the quaternary carbon at 96.4 ppm and a tertiary nitrogen at −161.5 ppm must be bonded to one another and the same carbon (at 96.4 ppm) bound to the aromatic carbocycle. (No other combinations are sensible, and only one H was shown to be N-bound, the pyrrole H.) This remarkable connection, in addition to the fused ring systems, gives rise to both the imide and the orthoamide functionalities. Neither of these functionalities appears to have been previously reported as being present in a natural product.

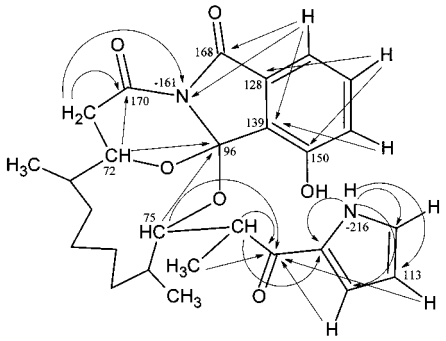

Figure 2. The decisive $^1H-\{^{13}C\}$ and $^1H-\{^{15}N\}$ long-range correlations leading to the structural elucidation of frankiamide. Also indicated are the chemical shifts of significant ^{13}C and ^{15}N nuclei.

Table 1. Accurate Mass Measurements by EI^+

m/z	rel int (%)	composition	found	calcd	deviation (ppm)
998	<2	$C_{54}H_{63}N_4O_{12}K$	998.4022	998.4080	5.8
982	<2	$C_{54}H_{63}N_4O_{12}Na$	982.4178	982.4340	16.5
480	<10	$C_{27}H_{32}N_2O_6$	480.2262	480.2260	0.3
321	5−10	$C_{20}H_{19}NO_3$	321.1369	321.1365	1.3
275	5−20	$C_{19}H_{17}NO$	275.1311	275.1310	0.3
162	10−55	$C_{10}H_{12}NO$	162.0915	162.0919	2.4
159	5−20	$C_9H_5NO_2$	159.0323	159.0320	1.7
133	30−40	C_8H_7NO	133.0530	133.0528	1.8
123	70−90	C_7H_9NO	123.0686	123.0684	1.1
94	100	C_5H_4NO	94.0290	94.0293	3.1

The mass spectra of **1** under EI^+ conditions is consistent with the structure provided by NMR. The presence of the pyrrole-containing side chain is confirmed by the formation of stable $C_7H_9NO^{+\bullet}$ (*m/z* 123) and $C_5H_4NO^+$ (*m/z* 94) ions. This latter ion represents the base peak, and the formation of this acylium cation is quite characteristic for acyl pyrroles.[20] Although the EI^+ spectrum of compound **1** varies greatly with experimental conditions (e.g., heating rate, final probe temperature, etc.) and the molecular ion is not always observed, there are several consistent fragment peaks that appear even at moderate heating of the probe and are suitable for accurate mass measurements (see Table 1) and the determination of metastable transitions (fragmentation patterns are depicted in Figure 3).

That the positive charge is mostly retained in the acyl pyrrole moiety accounts for the fragmentation of the polycyclic part of the molecule giving rise to only less prominent ions in the range of *m/z* 130−340. Of note though, consecutive losses of water (×3) and CO from the **A** fragment result in the formation of the fairly stable ion $C_{19}H_{17}NO^{+\bullet}$ (*m/z* 275), in which the polycyclic structure is presumably largely preserved as only one carbon atom is lost from the **A** fragment (Figure 3). The polycyclic structure is, however, cleaved at the later stages of fragmentation with the formation of $C_{10}H_{12}NO^+$ (*m/z* 162) and $C_9H_5NO_2^{+\bullet}$ (*m/z* 159) ions, which judging from their elemental compositions must be isoindolone-related structures.

What is remarkable about the EI^+ spectra of **1** is the presence of adducts (clusters) between the molecule and its alkaline salt, $[MS_{Na}]^{+\bullet}$ and $[MS_K]^{+\bullet}$ at *m/z* of 982 and

(19) Nurmi, K.; Ossipov, V.; Haukioja, E.; Pihlaja, K. *J. Chem. Ecol.* **1996**, *22*, 2023.

(20) Porter, Q. N. *Mass Spectrometry of Heterocyclic Compounds*, 2nd ed.; Wiley: New York, 1985; p 541.

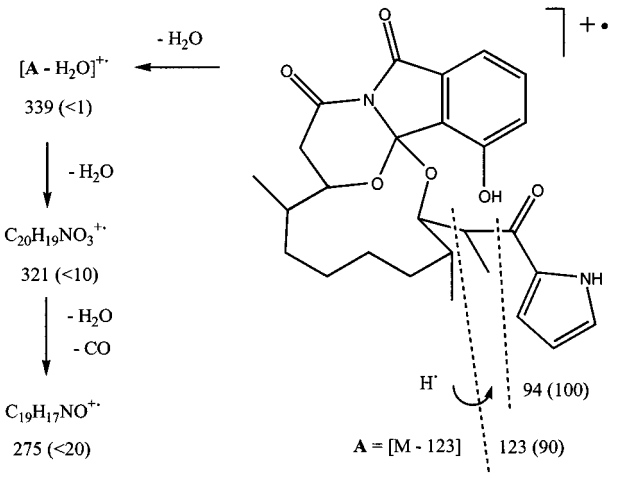

Figure 3. The MS fragmentation of **1** under EI^+ conditions. Numbers in parentheses represent the relative abundances of the fragment ions.

998, respectively (where $S_X = [M - H]^- X^+$, X = Na, K). Even cluster ions corresponding to $[M_2Na^+]$ and $[M_2K^+]$ at *m*/*z* 983 and 999, respectively, were also present, albeit at very low intensity. Many substances easily form stable multimolecular clusters under ESI and FAB conditions and the omnipresent alkali metal cations, Na^+ and K^+, are often incorporated, but to observe a similar phenomenon in EI^+ spectra is quite unusual. Given the structure of **1** elucidated by NMR, the propensity of **1** to form alkaline metal clusters and salts under various ionization conditions, though, can readily be rationalized. Both phenol and pyrrole functionalities permit salt formation, and the fused macrocyclic ring system together with the numerous potential ligand atoms (especially the 1,3-dicarbonyl fragment) and cleft positions facilitate the complexation. Nonetheless, despite the initial confusion, accurate mass measurements (Table 1) decidedly yielded an elemental composition of $C_{27}H_{32}N_2O_6$ (MW = 480) for the "unit", which was overwhelmingly consistent with the partial NMR formula of $C_{27}H_{\geq 30}N_2$.

As just evidenced by the EI^+ spectra, the MS of **1** was of a less than routine nature, and the ESI^+, ESI^-, and FAB^+ mass spectra of the sample (see Table 2) could each infer a different molecular weight for **1** if considered individually. The spectra from these three ionization modes contained clusters of prominent peaks with *m*/*z* values of up to 1100 (ESI^+), 1000 (ESI^-), and 1520 amu (FAB^+). Ions with *m*/*z* 503 and 525 were present in both ESI^+ and FAB^+ spectra (the spectra were otherwise dissimilar), which could correspond to $[MH]^+$ and $[MNa]^+$ ions for a substance with MW = 502, but this would not account for all the peaks present in the ESI spectra and, moreover, for the peaks at *m*/*z* 999 and 1517 in the FAB^+ spectrum. In particular, these latter two peaks implied that the molecular weight of **1** must not exceed 500 amu if they represent dimer and trimer cluster ions, respectively. The implicit contradictions of the $ESI^{+,-}$ and FAB^+ spectra were only resolved and their commonalties revealed by assessing the molecular weight of the substance as 480 amu and recognizing that **1** easily forms not only clusters with itself but also salts and adducts with alkaline metals (see Table 2). The molecular weight of 480 is also implicated by the presence of weak intensity ions at *m*/*z* 479 (ESI^-) and 481 (FAB^+) in addition to the *m*/*z* 480 ion (10% RI) present in the EI^+ spectrum.

Table 2. $ESI^{+,-}$ and FAB^+ Mass Spectra[a] of Frankiamide (1)

m/*z* (% rel int)			
ESI^+	ESI^-	FAB^+	composition
	479 (20)		$[M - H]^-$
		481 (3)	MH^+
	501 (100)		$[S_{Na}\text{-}H]^-$
503 (30)		503 (90)	MNa^+
		519 (70)	MK^+
525 (80)		525 (65)	$S_{Na}Na^+$
547 (50)			$S_{2Na}Na^+$
557 (80)			S_KK^+
	981 (60)		$S_{Na}[M - H]^-$ or $M[S_{Na} - H]^-$
	997 (55)		$S_K[M - H]^-$ or $M[S_K - H]^-$
		999 (100)	M_2K^+
		1005 (20)	$MS_{Na}Na^+$
		1021 (20)	$MS_{Na}K^+$ or MS_KNa^+
1037 (100)			MS_KK^+
1059 (50)			$2S_KNa^+$ or $S_{Na}S_KK^+$
1081 (35)			$S_{2Na}S_KK^+$
		1517 (10)	$2S_KMH^+$ or $S_KM_2K^+$

[a] S_{nX} denotes a salt, $[M - nH]^{-n}X^{+n}$, X = Na, K. Isotope ion peaks not included.

Thus, there are several remarkable features regarding compound **1**. Structurally it is very interesting in that it is a macrocycle with four fused rings containing an assortment of functional groups—pyrrole, phenol, ketone, imide, and orthoamide—together with six asymmetric centers. This combination of structural units results in some unusual behavior, namely, the dynamic equilibrium and, most peculiarly, the ready formation of adducts $[M_{1-3}Na(K)_x]^+$ under most MS conditions, including to some extent EI^+. The presence of imide and orthoamide groups are also unprecedented for a natural product. Further efforts will be directed toward the precise identification of the dynamic process at hand and X-ray crystallographic analysis for determination of the stereochemistry.

Experimental Section

***Frankia* Strain, Growth Conditions, and Isolation.** The *Frankia* AiPs1 strain used in this study was isolated from a stand of Finnish Scots pine (*Pinus sylvestris* L.) by inoculating axenic gray alder (*Alnus incana* L.) roots with soil suspensions and isolating the strain from the root nodules. On the basis of sequence similarity, the strain AiPs1 has been grouped in the *Alnus* host infection subgroup IIIb.[2] The isolated strain was then cultivated in PC-broth at 28 °C for about 8 weeks,[21,22] from which approximately 15 mg of ethyl acetate extractable material per liter of PC-culture broth was produced. After normal phase TLC (silica gel 60 F_{254}, water-saturated chloroform as eluent), the dry weight of the one active fraction (as determined by disk diffusion tests and testing for antimicrobial activity against *Brevibacillus laterosporus*) was 9 mg/L from which 5.2 mg of **1** was isolated by RP-TLC (RP-18 $WF_{254}S$, 46.2% methanol, 37.5% acetonitrile, and 16.4% water as eluent). This material was subsequently used directly for bioassays but was subjected to further purification by repetitive RP-HPLC prior to spectroscopic analysis. The addition of 2.5 mM Na_2HPO_4 to the HPLC eluent (otherwise the same eluent as for the RP-TLC was used) was necessary to obtain chromatographically well-behaved, sharp peaks. Compound **1** was then finally obtained as a colorless powder. Compound **1** was directly tested for antimicrobial activity against the following microbial strains: *Phytophthora* sp., *Heterobasidion* sp., *Fusarium* sp., *Botrytis* sp., *Rhizoctonia* sp., *Candida* sp., *Pseudomonas* sp., *Escherichia* sp., *Bacillus* sp., *Brevibacillus* sp., *Staphylococcus* sp., *Clavibacter* sp., *Entero-*

(21) Smolander, A.; Sarsa, M. L. *Plant Soil* **1990**, *122*, 129.
(22) Weber, A.; Smolander, A.; Nurmiaho-Lassila, E.-L.; Sundman, V. *Symbiosis* **1988**, *6*, 97.

coccus sp., and *Streptococcus* sp. using cell suspension assays for the bacteria and a modified disk diffusion method for the fungi. Of the 21 microbial strains tested, **1** showed significant inhibition toward nine of them. Furthermore, it was also tested for calcium antagonistic effects by measuring the $^{45}Ca^{2+}$ uptake via voltage-operated Ca^{2+} channels in clonal rat pituitary GH_4C_1 cells and was found to be comparable to verapamil hydrochloride. The experimental details and results of all these tests are fully described in the parallel report.[18]

General NMR and MS. NMR spectra were acquired at 500.16 MHz for ^1H, 125.78 MHz for ^{13}C, and 50.69 MHz for ^{15}N. The spectra were recorded at 25 °C, and both ^1H and ^{13}C spectra were referenced internally to tetramethylsilane (0 ppm for both) and ^{15}N spectra were referenced externally to 90% nitromethane in CD_3NO_2 (at 0 ppm). 1D spectra consisted of normal proton and carbon, nitrogen (acquired with single-pulse excitation and inverse-gated decoupling), DEPT 135°, selective INEPT (optimized on a $^nJ_{HC}$ of 2 Hz), and NOE difference measurements. 2D spectra comprised both phase-sensitive [DQF COSY, EXSY, and CHSHF ($^1H-\{^{13}C$ with partial homonuclear decoupling in f1 and optimized on a $^1J_{HC}$ coupling of 145 Hz)] and absolute-value mode variants [HSQC ($^1H-\{^{15}N\}$, optimized on a $^1J_{HN}$ coupling of 95 Hz) and HMBC ($^1H-\{^{13}C\}$, $^1H-\{^{15}N\}$, both optimized on a long-range coupling of 8 Hz for both $^nJ_{HC}$ and $^nJ_{HN}$)], mostly with field gradients. Spectral widths and resolution were appropriately optimized from the 1D spectra and generally processed with zero-filling (×2, ×4) and exponential weighting (plus a $2\pi/3$-shifted sinebell function for the absolute-value mode spectra) applied in both dimensions prior to Fourier transformation.

Mass spectra were acquired on a VG ZabSpec instrument for EI^+ and FAB^+ (*p*-nitrobenzyl alcohol as matrix) measurements using a direct insert probe. Accurate mass measurements in EI^+ mode were performed by peak matching technique using PFK as a reference substance with a resolution of 8000−10000 (at 10% peak height). $ESI^{+,-}$ (aqueous methanol by direct infusion or via HPLC inlet) measurements were acquired on a Sciex API 365 triple-quadrupole LC/MS/MS system. Masses were scanned from *m*/*z* 80 to 1100 amu in 0.3 amu steps. For negative (positive) ion measurements the needle voltage was set to −4100 (+5200) V, the orifice voltage to −35 (+45) V, and the ring voltage to −220 (+220) V. The sheath gas (nitrogen) temperature was set at 310 °C. Settings for MS-MS analyses were similar and utilized a collision energy of −25 (+20) V.

Frankiamide (1). ^1H NMR ($CDCl_3$, major conformer only) δ ppm: 13.533 (br. s, $\nu_{1/2} \approx 9$ Hz, H21); 8.297 (dd, $J_{H14} = 7.8$, $J_{H15} = 1.1$ Hz, H13); 7.649 (dd, $J_{H14} = 8.2$, $J_{H13} = 1.1$ Hz, H15); 7.474 (t, $J_{H13} = J_{H15} = 7.9$ Hz, H14); 7.410 (ddd, $J_{H23} = 3.1$, $J_{H21} = 2.3$, $J_{H24} = 1.3$ Hz, H22); 6.969 (ddd, $J_{H21} = 3.7$, $J_{H23} = 2.2$, $J_{H22} = 1.4$ Hz, H24); 6.239 (dt, $J_{H22} = 3.9$, $J_{H21} = J_{H24} = 2.2$ Hz, H23); 4.049 (dt, $J_{H9ax} = 11.5$, $J_{H9eq} = J_{H8} = 2.5$ Hz, H8a); 3.010 (dq, $J_{H2} = 10.0$, $J_{H25} = 6.7$, Hz, H18); 2.905 (d(sl AB)d, $J_{H9ax} = 13.0$, $J_{H8a} = 2.7$ Hz, H9eq); 2.804 (d(sl AB)d, $J_{H9eq} = 12.9$, $J_{H8a} = 11.8$ Hz, H9ax); 2.511 (dd, $J_{H18} = 10.0$, $J_{H3} = 2.1$ Hz, H2); 1.923 (m, H8); 1.50−0.65 [9H overlapped, approximate δ 1.35 and 1.25 (H4 pr., H5 pr., or H6 pr.); 1.35 and 1.05 (H4 pr., H5 pr., or H6 pr.); 2 × 1.13 (H4 pr., H5 pr., or H6 pr.); 1.08 (H3); 0.97 and 0.83 (H7 pr.)]; 0.843 (d, $J_{H8} = 7.01$ Hz, H27 Me); 0.735 (d, $J_{H18} = 6.6$ Hz, H25 Me); 0.734 (d, $J_{H3} = 6.9$ Hz, H26 Me). ^{13}C NMR ($CDCl_3$) δ ppm: 196.01 (s, C19); 170.32 (s, C10); 168.22 (s, C12); 150.11 (s, C16); 138.81 (s, C16a); 133.88 (s, C20); 129.18 (d, C22); 127.53 (d, C13); 126.86 (s, C12a); 124.95 (d, C14); 121.10 (d, C24); 112.87 (d, C15); 110.80 (d, C23); 96.39 (s, C16b); 75.28 (d, C2); 72.25 (d, C8a); 43.00 (d, C18); 32.20 (t, C9); 29.55 (t, C4, C5, or C6); 29.11 (t, C4, C5, or C6); 28.95 (d, C8); 26.68 (d, C3); 26.17 (t, C4, C5, or C6); 25.05 (t, C7); 11.61 (q, C25); 11.18 (q, C27); 9.72 (q, C26). ^{15}N NMR ($CDCl_3$) δ ppm: −161.45 (s, N11); −215.68 (d, N21).

Acknowledgment. Financial support from the Academy of Finland, grants no. 47231 (K.K.H. and J.P.H.) and 4284 (K.P.), is gratefully acknowledged.

Note Added in Proof. The imide functionality has been reported previously in natural products. See, for example: Viracaoundin, I.; Faure, R.; Gaydou, E. M.; Aknin, M. *Tetrahedron Lett.* **2001**, *42*, 2669.

JO001789Z